PAPER • **OPEN ACCESS**

Observation of semisolid deformation by using 4D-CT and 3DXRD

To cite this article: T Narumi *et al* 2020 *IOP Conf. Ser.: Mater. Sci. Eng.* **861** 012065

IOP Conf. Series: Materials Science and Engineering **861** (2020) 012065 doi:10.1088/1757-899X/861/1/012065

Observation of semisolid deformation by using 4D-CT and 3DXRD

T Narumi, T Nakata and H Yasuda

Department of Materials Science and Engineering, Kyoto University, Yoshida-honmachi, Sakyo, Kyoto, 606-8501 Japan

E-mail: narumi.taka.6n@kyoto-u.ac.jp

Abstract. Time-resolved X-ray tomography (4D-CT) and three-dimensional X-ray diffraction (3DXRD) were performed to investigate semisolid deformation in Al–10mass%Cu alloy. The configurations of solid grains were observed in-situ by 4D-CT and the crystallographic orientations of grains were also measured by 3DXRD. Translation and rotation of the solid grains in the semisolid are quantitatively analysed by the reconstructed 3D images and the diffraction spots. Based on the in-situ observation, we discuss about the motion of the solid grains and the formation of the shear band during the semisolid deformation.

1. Introduction

In various casting processes of metallic alloys, elimination of casting defects such as macrosegregation, porosity and hot tear is required for improving quality of castings and promoting efficiency of casting processes. It is of interest to study semisolid deformation in metallic alloys because the semisolid deformation occurs in various casting processes and is closely related to the formation of casting defects. The semisolid deformation can be driven by solidification shrinkage, external forces and thermosolutal convection during solidification. For example, the semisolid processing and the centrifugal casting generate the stress which influences the semisolid microstructure [1–3]. In common with granular materials, the rheological behaviour such as dilatancy was found in semisolid alloys [1, 2], which provides apparent volume expansion in response to shear deformation. Various studies about the rheology of semisolid alloys such as the mechanical and viscus behaviours, and the deformation of solid grains, have been reported. However, the change in the microstructure during the semisolid deformation has not been fully understood, which is essential to understand the formation mechanism of casting defects.

In-situ observation of solidification phenomena in various alloys has been performed by using X-ray imaging techniques at synchrotron radiation facilities. Thanks to the in-situ observations, quantitative analysis of dendrite growth / fragmentation / coarsening has been achieved [4–9]. In-situ observations proved that the massive-like δ–γ transformation rather than the peritectic solidification dominantly occurred in the conventional steels [10–15]. The growth behaviour of the spheroidal graphite in the ductile cast iron [16–19] were elucidated by the in-situ observation. These imaging techniques have also been applied to observe the semisolid deformation on a solid-grain scale. In the previous study, transmission (2D) observations of the semisolid deformation in thin Al–Cu alloys [20] and carbon steels [21] revealed that the local contraction and the dilation occurred in the semisolid alloys, and the shear deformation was localized during the deformation. The solid grains were mechanically isolated even at the high solid fraction ($f_s > 0.95$), and the rotation and the translation of the solid grains were dominant

during the semisolid deformation while the deformation of solid grains was modest. Therefore, to know the motion of the solid grains is essential to elucidate the semisolid deformation. However, by the 2D observation, the grain motion was restricted in the thin specimen (thickness was 200 μm), the liquid film existed between the grains and the sapphire specimen holders and the crystallographic orientation of the grains was difficult to measure. Hence, the 3D observation was necessary to obtain the grain motion during the semisolid deformation in the bulk specimen.

Recently, the 3D observation technique using time-resolved X-ray tomography (4D-CT) has been performed aiming to observe the time evolution and the spatial distribution of the solidifying microstructure in metallic alloys. The microstructural evolution such as the changes in the solid/liquid interfacial area and the curvature along with the solid fraction in specimens was extensively analysed [22–26]. 4D-CT has also worked for the semisolid deformation as well as the solidification phenomena. Spatial and time resolutions of 4D-CT allow to understand the translation of solid grains and the change in the local liquid fraction during the semisolid deformation [27, 28]. The liquation cracking of solid grains during the semisolid deformation was discovered by using 4D-CT, which leads to the structural refinement [29]. Using these techniques, the grain motion has been discussed mainly based on the grain translation during the semisolid deformation. For further development and understanding of the semisolid deformation, measurement of the grain rotation in 3D, which provides the semisolid deformation in addition to the translation, is desired. To analyse the grain rotation, the change in crystallographic orientation of each solid grain during the semisolid deformation at high temperature is required.

3DXRD is a non-destructive method to measure the crystallographic orientation of each grain during deforming and phase-transforming specimens [30–32]. We aimed to analyse the 3D grain motion by measuring the rotation using 3DXRD in addition to the translation using 4D-CT. The observation results are expected to contribute further understanding the 3D grain motion during the semisolid deformation. This paper demonstrates the 3D grain motion in Al–10mass%Cu alloys with diameter of 1 mm during semisolid deformation by using the 4D-CT and 3DXRD technique developed by our group. We also discuss about the motion of the solid grains and formation of the shear band during the semisolid deformation.

2. Experimental method

The measurement of 4D-CT and 3DXRD was performed at beamline BL20XU of SPring-8 (synchrotron radiation facility in Hyogo, Japan). Figure 1 shows the schematic illustrations of 4D-CT and 3DXRD, respectively. To perform 4D-CT, the monochromatized X-ray (37.7 keV, approximately 5 mm in width and 3 mm in height) was applied to a specimen rotated at 4 s/rotation. The transmission images were obtained by a beam monitor, ORCA-Flash (1024 × 1024 pixels, pixel size 6.5 μm × 6.5 μm, Hamamatsu Photonics) at 100 fps. Three-dimensional images were reconstructed by using 200 transmission images over 180 degrees rotation. The voxel size of reconstructed images was 6.5 μm × 6.5 μm × 6.5 μm. To perform 3DXRD with vertical resolution, the slit X-ray whose height was 100 μm was applied repeatedly from the top to the bottom of the rotating specimen divided into 20 layers, which took 15 s in each diffraction measurement. The diffraction spots of the solid grains in the semisolid specimen were detected by a X-ray flat panel sensor (1008 × 682 pixels, pixel size 100 μm × 100 μm, Hamamatsu Photonics) at 30 fps. Diffractions from all solid grains, whose number was 10–20, in the field of view were detected using diffraction images over 360 degrees rotation. In the present research, both diffractions of Al {111} and Al {200} were employed to determine the crystallographic orientations of the solid grains. By the distortion of the diffraction spots from the circles centred at the direct X-ray beam according to the position of the solid grains, the horizontal resolution of 3DXRD was provided.

Al–10mass%Cu alloy was used as the specimen. The specimen which had the rod-like shape (2 mm in diameter and 4 mm in length) with the reduced section in the middle (1.4 mm in diameter) to localize deformation in the observation field, was inserted into a sintered Al_2O_3 pipe (ID 2.0 mm, OD 3.0 mm). The eutectic structure of α-Al and θ-Al_2Cu in the specimen was melted and maintained at above the eutectic temperature for 15 min in a vacuum atmosphere (approximately 1 Pa) to make the semisolid

specimen isothermal before applying deformation. The eutectic temperature was determined from the disappearance of the diffraction spots of θ-Al_2Cu {211}. The compression deformation of the specimen was applied intermittently three times by pushing down an Al_2O_3 rod placed on the top of the specimen (each deformation period is described as #1, #2 and #3 hereinafter). The deformation lengths of #1, #2 and #3 were 129 μm, 228 μm and 456 μm, respectively, and the deformation rate in each compression, which was calculated from the specimen length and the velocity of the Al_2O_3 rod, was about 10^{-4} /s. The condition of the specimen during the experiment was continuously observed by the transmission images. At each deformation period, 4D-CT and 3DXRD were performed. Figure 2 shows transmission images of the semisolid specimen of whole observation area for 4D-CT, and the diffraction spots obtained from the represented area (slit area) for 3DXRD as an example. Using the data obtained by the in-situ observation, quantitative analysis of the semisolid deformation including the crystallographic orientation of solid grains was performed.

3. Results and discussion

Figure 3 shows the 3D reconstructed images of the solid grains in the observation area of the specimen from the initial to #3. The colour variation of the solid grains represents the individual grains. The solid grains were distributed uniformly in the semisolid specimen before the deformation. This indicates that no macrosegregation such as the band segregation existed in the specimen. Once deformation was applied to the specimen, the impingement between the solid grains and the rearrangement of the solid grains occurred, resulting in the formation of the shear band indicated as the white arrows in figure 3.

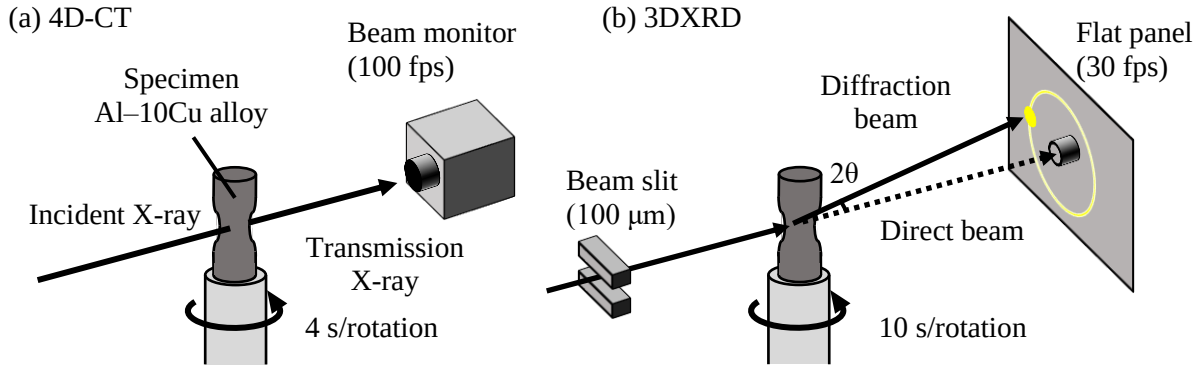

Figure 1. Schematics illustration of (a) 4D-CT and (b) 3DXRD.

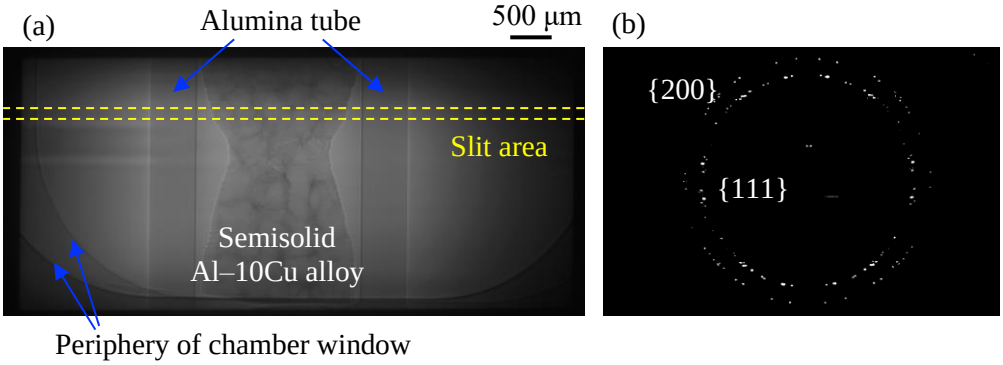

Figure 2. (a) Transmission image of the specimen (the slit beam irradiated the area between the dashed lines), and (b) diffractions obtained from the slit area in (a).

For considering the details of the microstructural evolution during the deformation, the vertical and the horizontal cross-sections which contain the shear band were extracted as shown in figure 4. The bright and dark contrast represent the solid and liquid phase, respectively. Several porosities were observed near the constricted part of the specimen as shown black areas in figure 4. The intergranular liquid films were accumulated with the rearrangement of the solid grains by applying the deformation. The shear band was confirmed in the upper half of the observation area. The shear band tilted from the vertical axis of the specimen (z-axis) whose direction was parallel to the compression direction. This indicates that the solid grains complexly displaced by the impingement between the solid grains instead of the simple translation toward the z-axis. To investigate the correlation of the translation of the solid grains with the formation of the shear band, we define a new coordinate system in which y'-axis is in common with the original y-axis, and x'-axis and z'-axis are perpendicular and parallel to the shear band, respectively. Figure 5 shows the relative translations of the solid grains from the initial to #3 near the shear band using the new coordinate system. Here, the translation was analysed from the movement of centre of mass in the solid grains by using the reconstructed images of 4D-CT. Since those solid grains moved opposite directions, they were classified as group A and group B in accordance with their translational directions. As shown in figure 5, group A (the outer grains) moved larger than group B (the inner grains). The cause of the translation difference between group A and group B was unclear from the grain motion in the observation field. In this observation, there is the possibility that the grains outside of the observation field interacted with group A and group B.

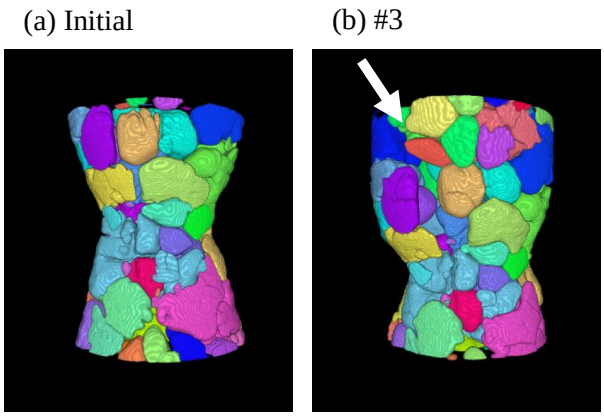

Figure 3. 3D reconstructed images of semisolid Al–10mass%Cu alloy (white arrows indicate the shear band); (a) initial and (b) #3.

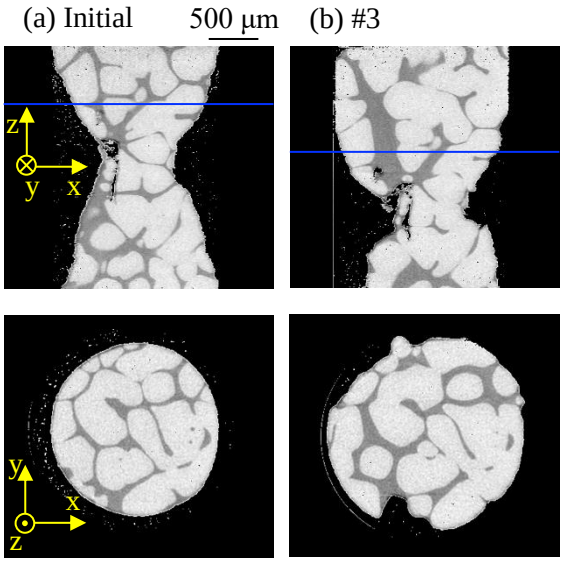

Figure 4. 2D extracted images from 3D images of semisolid Al–10mass%Cu alloy; blue lines in the vertical cross-sections indicate the position of the horizontal cross-sections; (a) initial and (b) #3.

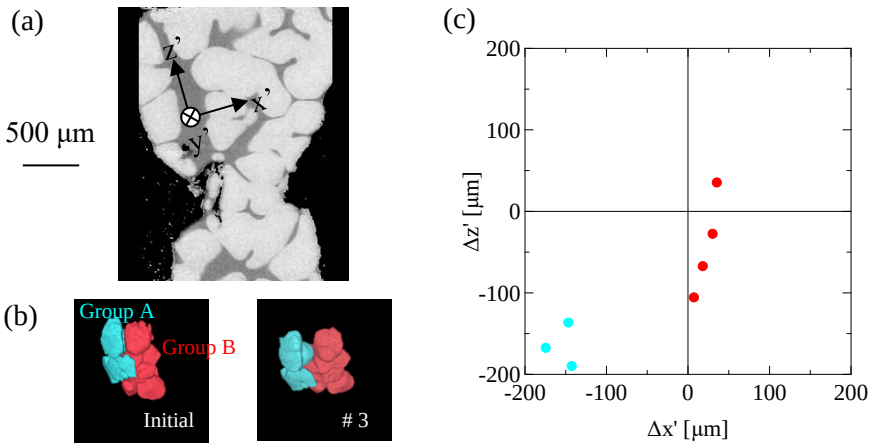

Figure 5. (a) definition of the new coordinate along with the shear band, (b) the solid grains near the shear band at initial and at #3; the number of the solid grains in group A (blue) and group B (red) were three and four, respectively, and (c) the translation length of each grain in group A (blue) and group B (red) from the initial to #3 in the new coordinate of x'-z' plane.

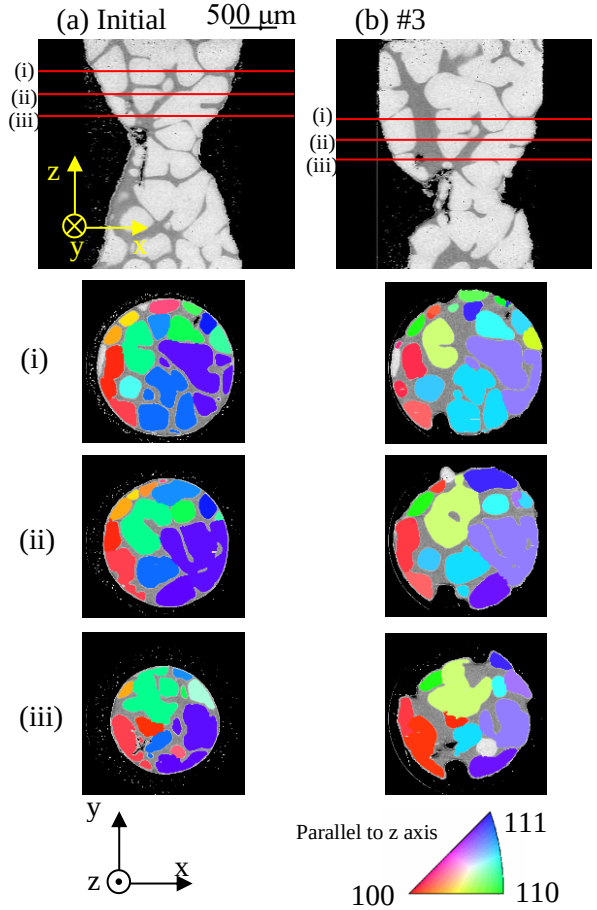

Figure 6. Vertical cross-sections and inverse pole figures of the horizontal cross-sections indicated as (i), (ii) and (iii); (a) initial and (b) #3.

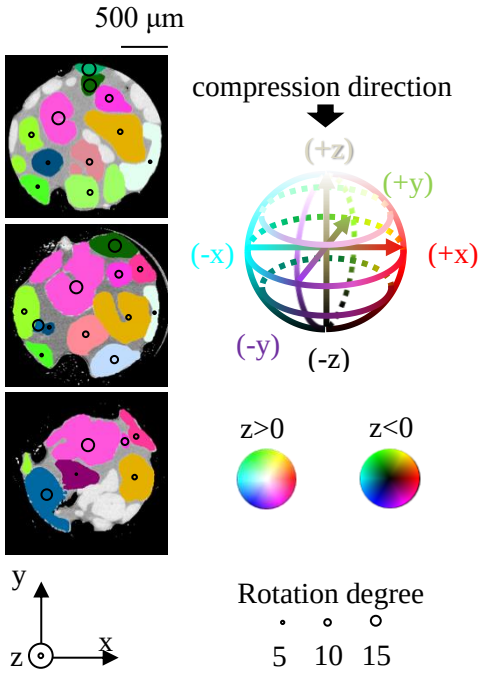

Figure 7. Change in the rotational direction and the degree of rotation from initial to #3; the colour variations and the circles indicates the rotational direction and the degree of rotation, respectively.

Figure 6 shows the inverse pole figure of the solid grains in the horizontal cross section marked in figure 4. The crystallographic orientation analysis of the solid grains in the semisolid alloy was achieved by 3DXRD at each deformation period, though a few grains were unavailable due to their smaller size and weaker diffraction intensity. Using those inverse pole figures, the grain rotation was assessed as shown in Figure 7. Here, the colour variation represents the both of the rotational axis direction and rotative direction obtained by 3DXRD. The rotational axis direction was defined as the tilt angle form z-axis and represented by x-y coordinate. The rotative direction was defined as positive (+z) when a solid grain rotated clockwise as viewed from the top of the specimen. The circles placed in the grains represent the degree of rotation. From figure 7, the solid grains rotated randomly, and no apparent tendency was confirmed. To investigate the correlation among the grain motion and the grain size near the shear band, the translation length, the degree of rotation and the volume of the solid grains from initial to #3 were evaluated based on 4D-CT and 3DXRD, and shown in figure 8. The region near the shear band (figure 8 (a)), two grains were larger than 0.20 mm^3 and the other grains were 0.02–0.06 mm^3. The distribution of the translation length represents that the solid grains moved ununiformly and the grain rearrangement occurred. No apparent tendencies were found between the translation, the rotation and the volume of the solid grains in this study (from figure 8(a)). To elucidate the relationship between the formation of the shear band and the rearrangement of the solid grain, observing the motion of large number of grains from the semisolid specimen and treating those data statistically are necessary.

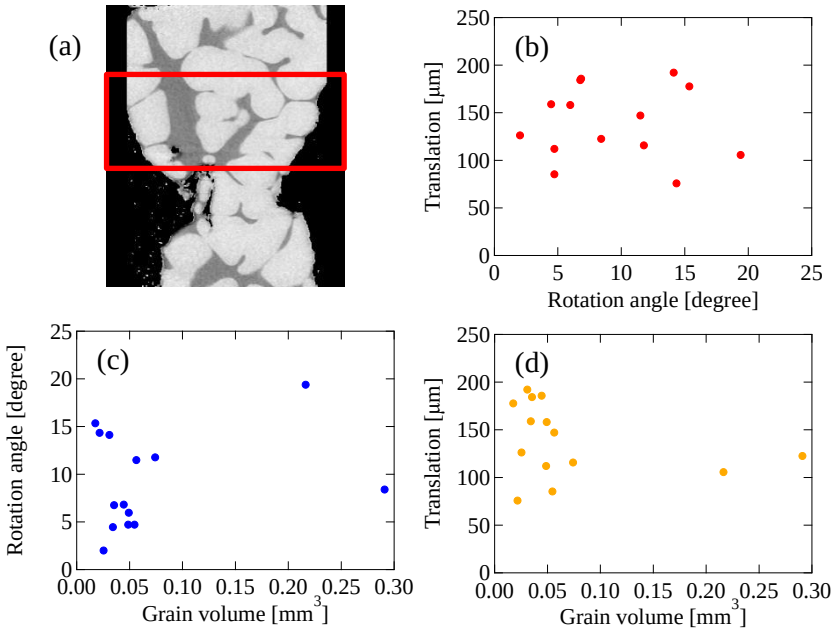

Figure 8. (a) The analysed region in the semisolid specimen, and the correlation between (b) translation and rotation angle, (c) rotation angle and grain volume, and (d) translation and grain volume.

4. Conclusion

In this study, 4D-CT and 3DXRD were performed for in-situ observation of semisolid deformation in a bulk specimen of Al–10mass%Cu alloy. The translation and rotation of the solid grains in the observation area were quantitatively analysed by the 3D reconstructed images and diffraction spots in synchronization with the sample rotation, respectively. As the compression deformation was applied to the semisolid specimen, the formation of the shear band was obtained. The translation of the solid grains was measured by the reconstructed images of 4D-CT. The solid grains in both side of the shear band moved apart each other due to the interaction between the solid grains. The rotation of the solid grains was also measured by 3DXRD. No apparent tendency of the grain rotation was obtained. The interaction between grains essentially caused the translation motions of solid grains and the rotation motion occurred as a result of the translation. The random rotation suggested that the forces causing the translation rather than the rotation should be included in a semisolid-deformation model.

We concluded that the motions of the solid grains during the semisolid deformation are analysed quantitatively based on the in-situ observations using 4D-CT and 3DXRD. For the statistical elucidation of the interaction between the solid grains during the semisolid deformation, it is of interest to study the semisolid deformation in a bulk specimen containing more than 1000 grains.

Acknowledgement

Part of this study was supported by a Grant-in-Aid for Scientific Research (S) (Grant Number 17H06155) from MEXT, Japan. The synchrotron radiation experiments were performed as general projects at a beamline of BL20XU at SPring-8 (JASRI) 2019A1400.

References

[1] Gourlay C M and Dahle A K 2007 *Nature* **445** 70–3
[2] Gourlay C M, Meylan B and Dahle A K 2008 *Acta Mater.* **56** 3403–13
[3] Kang I and Ohnaka I 1997 *J. Japan Foundry Eng. Soc.* **69** 119–26
[4] Mathiesen R H, Arnberg L, Mo F, Weitkamp T and Snigirev A 1999 *Phys. Rev. Lett.* **83** 5062–5
[5] Yasuda H, Ohnaka I, Kawasaki K, Sugiyama A, Ohmichi T, Iwane J and Umetani K 2004 *J. Cryst. Growth* **262** 645–52
[6] Mangelinck-Noël N, Nguyen-Thi H, Reinhart G, Schenk T, Cristiglio V, Dupouy M-D, Gastaldi J, Billia B, Härtwig J and Baruchel J 2005 *J. Phys. D. Appl. Phys.* **38** A28–32
[7] Li B, Brody H D, Black D R, Burdette H E and Rau C 2006 *J. Phys. D. Appl. Phys.* **39** 4450–6
[8] Yasuda H *et al.* 2008 *Int. J. Cast Met. Res.* **21** 125–8
[9] Yasuda H et al. 2009 Int. J. Cast Met. Res. **22** 15–21
[10] Yasuda H *et al.* 2011 *IOP Conf. Ser. Mater. Sci. Eng.* **27** 0–9
[11] Yasuda H *et al.* K 2012 IOP Conf. Ser. Mater. Sci. Eng. **33**
[12] Nishimura T, Morishita K, Nagira T, Yoshiya M and Yasuda H 2015 *IOP Conf. Ser. Mater. Sci. Eng.* **84** 012062
[13] Nishimura T, Morishita K, Yoshiya M, Nagira T and Yasuda H 2019 *Tetsu-to-Hagane* **105** 290–8
[14] Nishimura T, Matsubayashi R, Morishita K, Yoshiya M, Nagira T and Yasuda H 2019 *ISIJ Int.* **59** 459–65
[15] Yasuda H, Morishita K, Nakatsuka N, Nishimura T, Yoshiya M, Sugiyama A, Uesugi K and Takeuchi A 2019 *Nat. Commun.* **10** 3183
[16] Yamane K *et al.* 2014 J. Japan Foundry Eng. Soc. **86** 461–70
[17] Chatchari K, Akira S, Kouhei M and Hideyuki Y 2018 *J. Japan Foundry Eng. Soc.* **90** 602–12
[18] Yasuda H, Sugiyama A, Kiattisaksri C, Morishita K, Nagira T, Yoshiya M, Uesugi K and Takeuchi A 2018 *Mater. Sci. Forum* **925** 104–9
[19] Bjerre M K, Azeem M, Lee P D, Hattel J H and Tiedje N S 2018 **925** 118–24
[20] Gourlay C M, Dahle A K, Nagira T, Nakatsuka N, Nogita K, Uesugi K and Yasuda H 2011 *Acta Mater.* **59** 4933–43

[21] Nagira T *et al.* 2011 *Scr. Mater.* **64** 1129–32
[22] Ludwig O, Dimichiel M, Salvo L, Suéry M and Falus P 2005 *Metall. Mater. Trans. A* **36** 1515–23
[23] Aagesen L K, Fife J L, Lauridsen E M and Voorhees P W 2011 *Scr. Mater.* **64** 394–7
[24] Gibbs J W, Mohan K A, Gulsoy E B, Shahani A J, Xiao X, Bouman C A, De Graef M and Voorhees P W 2015 *Sci. Rep.* **5** 11824
[25] Puncreobutr C, Phillion A B, Fife J L and Lee P D 2014 *Acta Mater.* **64** 316–25
[26] Yasuda H, Kawarasaki T, Tomiyori Y, Kato Y and Morishita K 2019 *IOP Conf. Ser. Mater. Sci. Eng.* **529** 012023
[27] Terzi S *et al.* 2009 *Scr. Mater.* **61** 449–52
[28] Sistaninia M, Terzi S, Phillion A B, Drezet J-M and Rappaz M 2013 *Acta Mater.* **61** 3831–41
[29] Karagadde S *et al.* 2015 *Nat. Commun.* **6** 8300
[30] Jensen D J, Lauridsen E M, Margulies L, Poulsen H F, Schmidt S, Sørensen H O and Vaughan G B M 2006 *Mater. Today* **9** 18–25
[31] Offerman S E, van Dijk N H, Sietsma J, Lauridsen E M, Margulies L, Grigull S, Poulsen H F and van der Zwaag S 2006 *Nucl. Instruments Methods Phys. Res. Sect. B Beam Interact. with Mater. Atoms* **246** 194–200
[32] Toda H, Ohkawa Y, Kamiko T, Naganuma T, Uesugi K, Takeuchi A, Suzuki Y and Kobayashi M 2013 *Acta Mater.* **61** 5535–48